

DISTINGUISHING ALK+ ANAPLASTIC LARGE CELL LYMPHOMA (ALCL) AND ALK+ LBCL CAN BE CHALLENGING

Most ALK+ LBCL are CD30-negative/weak, whereas ALK+ ALCL are strongly and uniformly CD30 positive, making the differential diagnosis theoretically very simple. Nevertheless, as seen in the present case, strong uniform CD30 expression is possible in ALK+ LBCL.⁶ Together with an absence of significant expression of common B cell markers (CD20, PAX-5, CD79a) and strong expression of CD4 and cytotoxic molecules, this may lead to a misdiagnosis of ALK+ ALCL, especially in the presence of an NPM-ALK rearrangement (more characteristic of ALK+ ALCL). A useful hint to the correct diagnosis lies in cell morphology: it is mainly immunoblastic/plasmablastic in ALK+ LBCL and highly pleomorphic, often with 'hallmark' forms in ALK+ ALCL. Hence, when confronted with atypical features in an ALK+ tumour, determining the right lineage (B or T/NK) by additional immunohistochemical and/or molecular studies is key to the correct diagnosis. It is also worth noting that this distinction is not purely academic, as the two entities have a different prognosis and are treated differently.⁶

Acknowledgements

The authors would like to thank Julien Mezghani, Marie H el ene Delfau-Larue and Thierry Molina.

Conflicts of interest

The authors declare that there are no conflicts of interest.

Data availability statement

Data sharing not applicable to this article as no datasets were generated or analysed during the current study.

Josette Briere¹
Emmanu le Lechapt^{1,8}
Phillippe Gaulard^{1,8}

¹Department of Pathology, University Hospital Henri Mondor, AP-HP, Cr eteil, France, ²Portuguese Institute of Oncology, Porto, Portugal, ³Department of Neuropathology, GHU Paris, Psychiatry and Neuroscience, Sainte-Anne Hospital, Paris, ⁴UMR S1266, INSERM, IMA-BRAIN, Institut de Psychiatrie et Neurosciences de Paris (IPNP), Paris, France, ⁵Universit  de Paris, Paris, France, ⁶Medipath laboratory, Paris, France, ⁷Department of Pathology, Henri Becquerel Center, Rouen, France, ⁸IMRB, Inserm U955, Faculty of Medicine, University of Paris-Est Cr eteil, Cr eteil, France



References

1. Calvani J, G erard L, Fadlallah J *et al*. A comprehensive clinicopathologic and molecular study of 19 primary effusion lymphomas in HIV-infected patients. *Am. J. Surg. Pathol.* 2022; **46**: 353–362.
2. Pan Z, Hu S, Li M *et al*. ALK-positive large B-cell lymphoma: a clinicopathologic study of 26 cases with review of additional 108 cases in the literature. *Am. J. Surg. Pathol.* 2017; **41**: 25–38.
3. Garcia-Reyero J, Martinez Magunacelaya N, Gonzalez de Villambrosia S *et al*. Genetic lesions in MYC and STAT3 drive oncogenic transcription factor overexpression in plasmablastic lymphoma. *Haematologica* 2021; **106**: 1120–1128.
4. Huettl KS, Staiger AM, Horn H *et al*. Cytokeratin expression in plasmablastic lymphoma – a possible diagnostic pitfall in the routine work-up of tumours. *Histopathology* 2021; **78**: 831–837.
5. Wei P, Jin M, Jiang L, Wang Y, Xie J, Hu X. Anaplastic lymphoma kinase-positive large B-cell lymphoma with a diagnostic pitfall of carcinoma: a case report. *Int. J. Clin. Exp. Pathol.* 2017; **10**: 11219–11224.
6. Mehra V, Pomplum S, Ireland R *et al*. ALK-positive large B-cell lymphoma with strong CD30 expression; a diagnostic pitfall and resistance to brentuximab and crizotinib. *Histopathology* 2016; **69**: 880–882.

Coronavirus hunted in human pneumocytes and alveolar macrophages: a case report

DOI: 10.1111/his.14637

A number of pathological studies of coronavirus disease 2019 (COVID-19) autopsied tissues have been published. The results commonly show that severe acute respiratory syndrome coronavirus 2 (SARS-CoV-2) mainly infects lung tissues, as supported by the detection of the viral genome and antigens in pneumocytes and alveolar macrophages.¹ There have

Sara Petronilho^{1,2} 
Viviane Gournay¹
Arnault Tauziede-Espariat^{3,4,5,6} 
H elo se Pina¹
Adrien Pecriaux¹
Fanny Drieux⁷
Elsa Poullot^{1,8}

also been several reports of transmission electron microscopy (TEM) evidence of SARS-CoV-2 infection in patient specimens, but it is controversial as to whether real viral particles were observed.^{2,3}

In this study, we used TEM to observe SARS-CoV-2 (B.1.1.7, alpha) particles and intracellular structures associated with viral infection in type II pneumocytes and alveolar macrophages in COVID-19 autopsied lung tissue, and clarified the differences between the two cell types.

A 64-year-old woman (body mass index of 31) with COVID-19 was admitted to the hospital with severe general fatigue. During admission, she had no

fever or respiratory symptoms, but her creatinine kinase and troponin I levels were high. After 9 h, she developed chest pain and ventricular fibrillation, and she died within 72 h. We suspected fulminant myocarditis. Autopsy indicated mild myocarditis and marked pulmonary congestion with rare hyaline membrane formation. SARS-CoV-2 RNA was detected at low titres in the heart and at high levels ($>10^7$ copies/ μg RNA) in the lungs. Enzyme-antibody double immunostaining revealed SARS-CoV-2 nucleoprotein (NP) antigens in epithelial membrane antigen-positive type II pneumocytes and CD68-positive alveolar macrophages (Figures 1A and 2A).

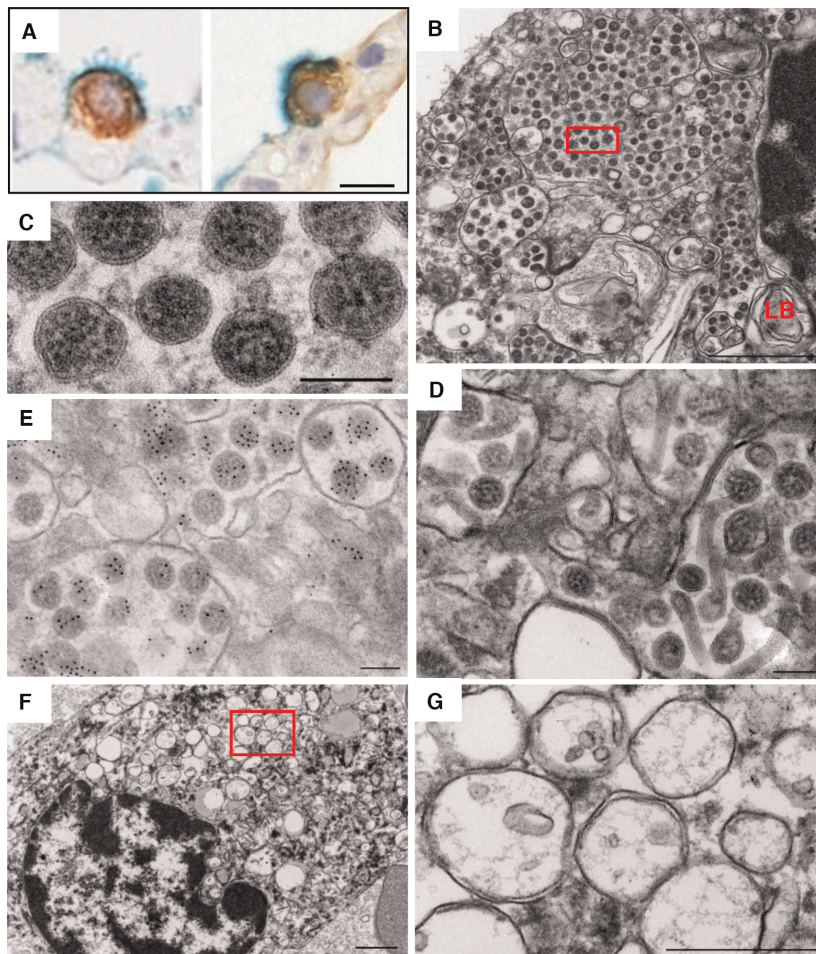


Figure 1. Severe acute respiratory syndrome coronavirus 2 (SARS-CoV-2) particles in type II pneumocytes. **A**, Double staining with antibodies against SARS-CoV-2 nucleoprotein (NP) antigens and epithelial membrane antigen (EMA). SARS-CoV-2 NP antigens (brown) are positive in the EMA-positive pneumocytes (green). Scale bar: 10 μm . **B**, Numerous virus particles are visible in the large vesicles within the cytoplasm of type II pneumocytes. Scale bar: 1 μm . **C**, Higher magnification of the red boxed area in (B). Scale bar: 100 nm. **D**, Tubular structures are observed together with viral particles in vesicles within the cytoplasm of type II pneumocytes. Scale bar: 100 nm. **E**, Immunogold labelling of SARS-CoV-2 particles with a rabbit antibody against SARS-CoV-2 NP antigens and a donkey anti-rabbit immunoglobulin conjugated to 6-nm gold particles. Scale bar: 100 nm. **F**, A region of double-membrane vesicles, which constitute a common feature of coronavirus-infected cells. Scale bar: 1 μm . **G**, Higher magnification of the red boxed area in (F) showing the presence of thin and electron-dense filaments in the double-membrane vesicles. Scale bar: 500 nm. LB, lamellar body.

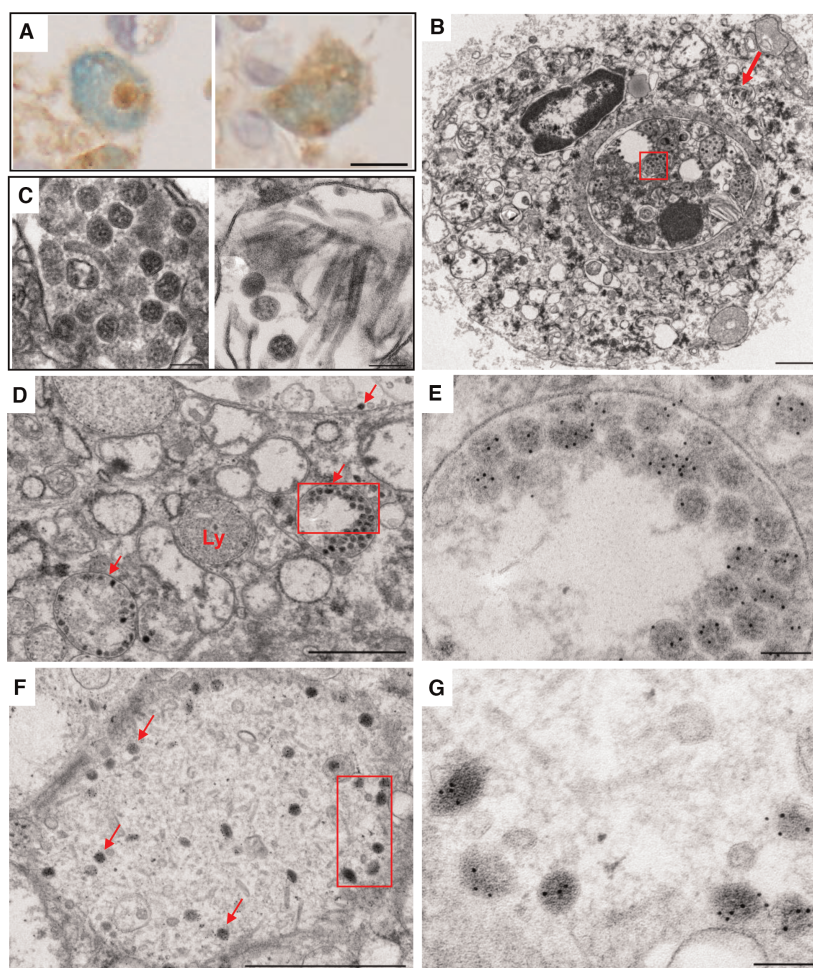


Figure 2. Severe acute respiratory syndrome coronavirus 2 (SARS-CoV-2) particles in alveolar macrophages. **A**, Double staining with antibodies against SARS-CoV-2 nucleoprotein (NP) antigens and CD68. SARS-CoV-2 NPs (brown) are positive in the CD68-positive alveolar macrophages (green). Viral antigens are localized in one cytoplasmic region of the macrophages (left) or diffusely detected in the cytoplasm (right). Scale bar: 10 μ m. **B**, Phagocytosis of an infected cell in an alveolar macrophage. Scale bar: 1 μ m. **C**, Left: high magnification of the red boxed area in (B) showing viral particles and tubular structures within a phagocytosed type II pneumocyte. Scale bar: 100 nm. Right: high magnification of the area indicated by the red arrow in (B) showing vesicles and tubular structures containing viral particles within the cytoplasm of the macrophage. Scale bar: 100 nm. **D**, Immunological labelling of SARS-CoV-2 particles in alveolar macrophages. Several viral particles are visible in the vesicles within the alveolar macrophage cytoplasm (red arrows). Scale bar: 1 μ m. **E**, Higher magnification of the red boxed area in (D) showing the presence of gold particles (6 nm) on the virus particles. Scale bar: 100 nm. **F**, Sparse viral particles in the large vesicles of alveolar macrophages (red arrows). Scale bar: 1 μ m. **G**, Higher magnification of the red boxed area in (F) showing the presence of gold particles (6 nm) on the oval virus particles. Scale bar: 100 nm. Ly, lysosome.

In type II pneumocytes, TEM analysis revealed many coronavirus particles within a large cytoplasmic vesicle (diameter of 1.73 μ m) (Figure 1B). The diameter of the viral particles averaged 78.2 nm, excluding spikes (Figure 1C). Within the viral particles, small electron-dense spots (average diameter of 8.6 nm), reflecting cross-sections through the helical nucleocapsids, were clearly observed (Figure 1C). Smaller cytoplasmic vesicles (average diameter of 258 nm), containing approximately 5–20 virus particles (Figure 1D), were observed more frequently than

larger vesicles (Figure 1B). The viral particles were confirmed by the use of immunogold electron microscopy (EM) with an antibody against SARS-CoV-2 NP antigens (Figure 1E). No viral particles were found outside the vesicles, as previously reported.³ It is noted that tubular structures (average diameter of 30 nm) were observed together with virus particles in the smaller vesicles (Figure 1D). Goldsmith *et al.*⁴ reported similar tubular structures in the vesicles of SARS-CoV-infected cultured cells. Here, for the first time, we confirmed the presence of the same

structure in SARS-CoV-2-infected human lung tissue. In addition, double-membrane vesicles (DMVs), which are formed during coronavirus replication and derived from the endoplasmic reticulum of the host cell, were observed in type II pneumocytes (Figure 1F,G). The average diameter of the DMVs was 324 nm, which is consistent with that observed in SARS-CoV-2-infected VeroE6 cells.⁵ Thin and electron-dense filaments, presumably representing viral RNA, were clearly observed in the DMVs (Figure 1G).

It is still unclear whether the alveolar macrophages test positively for viral antigens and/or viral RNA because they phagocytose viral particles or because they are infected with SARS-CoV-2. In studies of *in-vitro* infection, human monocyte-derived macrophages can be infected with SARS-CoV-2, but they fail to support the production of progeny virus.⁶ In double immunostaining of alveolar macrophages, viral antigens were often detected localized to a small portion of the cytoplasm (Figure 2A, left panel), and, rarely, some were detected diffusely (Figure 2A, right panel). Corresponding with this observation, TEM revealed alveolar macrophages phagocytosing type II pneumocytes (Figure 2B,C). The phagocytosed type II alveoli had vesicles containing numerous viral particles and tubular structures (Figure 2B,C, left panel), whereas, in the cytoplasm of the macrophage, a vesicle with a few viral particles and tubular structures was observed (Figure 2C, right panel). The particles in the vesicles (Figure 2D) were identified as SARS-CoV-2 by the use of immunogold EM (Figure 2E). Some macrophages showed large vesicles with sparse SARS-CoV-2 particles, some of which were irregularly shaped (Figure 2F,G). DMVs were not found in the alveolar macrophages.

A limitation of this study was that the findings were based on a single case. Nonetheless, differences in the presence of virus particles in type II pneumocytes and in alveolar macrophages were directly shown by TEM. Alveolar macrophages showed phagocytosis of infected cells, but did not show evidence of active viral replication, such as DMVs, and the amount of viral particles in macrophages was much lower than that in pneumocytes. The tubular structures, which were found in this case and have been reported in cultured cells, are suspected to be related to coronavirus infection, but require further case series and detailed studies.

Conflicts of interest

The authors declare no conflicts of interest. The study sponsor(s) had no role in the study design, in the

collection, analysis and interpretation of data, in the writing of the report, or in the decision to submit the report for publication.

Ethics approval

The study complied with the ethical standards of the Ethical Review Committee for Medical Research Involving Human Subjects, National Institute of Infectious Diseases (approval No. 1178, 3 September 2020). Written informed consent was obtained from the patient's family for the publication of the data and accompanying images.

Author contributions


M. Kataoka and N. Nakajima contributed to the analysis of the pathological findings and drafted the manuscript. Y. Tajima provided clinical information. T. Tsukamoto and Y. Tajima performed the autopsy and collected the samples. M. Kataoka contributed to the EM analysis. Y. Sato contributed to the histological analysis. H. Katano contributed to next-generation sequencing. M. Kataoka, Y. Sato, T. Suzuki and N. Nakajima contributed to the data interpretation. All authors have reviewed and approved the final version of the manuscript.



Acknowledgements

We thank Dr Miyamoto for technical advice on immunogold EM. This study was supported in part by the Ministry of Education, Culture, Sports, Science and Technology (MEXT) of Japan with a grant to N. Nakajima under grant number 20 K07400, and by Grants-in-Aid from the Japan Agency for Medical Research and Development (AMED) to T. Suzuki under grant number JP21fk0108104.

Data availability statement

SARS-CoV-2 sequence results was registered in the Global Initiative on Sharing All Influenza Data (GISAID, <https://www.gisaid.org/>, accession no. EPI_ISL_3541226).

Michiyo Kataoka¹ 
 Tetsuya Tsukamoto²
 Yasuhisa Tajima³
 Yuko Sato¹

Harutaka Katano¹ 
Tadaki Suzuki¹
Noriko Nakajima¹ 

¹Department of Pathology, National Institute of Infectious Diseases, Shinjuku, Japan, ²Department of Diagnostic Pathology, Fujita Health University School of Medicine, Toyoake, Japan, ³Department of Infectious Diseases, Hamamatsu Medical Center, Hamamatsu, Japan

References

1. Martines RB, Ritter JM, Matkovic E *et al.* Pathology and pathogenesis of SARS-CoV-2 associated with fatal coronavirus disease, United States. *Emerg. Infect. Dis.* 2020; **26**: 2005–2015.
2. Hopfer H, Herzig MC, Gosert R *et al.* Hunting coronavirus by transmission electron microscopy—A guide to SARS-CoV-2-associated ultrastructural pathology in COVID-19 tissues. *Histopathology.* 2021; **78**: 358–370.
3. Bullock HA, Goldsmith CS, Zaki SR, Martines RB, Miller SE. Difficulties in differentiating coronaviruses from subcellular structures in human tissues by electron microscopy. *Emerg. Infect. Dis.* 2021; **27**: 1023–1031.
4. Goldsmith CS, Tatti KM, Ksiazek TG *et al.* Ultrastructural characterization of SARS coronavirus. *Emerg. Infect. Dis.* 2004; **10**: 320–326.
5. Klein S, Cortese M, Winter SL *et al.* SARS-CoV-2 structure and replication characterized by in situ cryo-electron tomography. *Nat. Commun.* 2020; **11**: 5885.
6. Jian Z, Yuhang W, Li K, David KM, Chantal A, Stanley P. Severe acute respiratory syndrome coronavirus 2-induced immune activation and death of monocyte-derived human macrophages and dendritic cells. *J Infect Dis.* 2021; **223**: 785–795.